Int. J. Electrochem. Sci., 8 **(2013)** 3349 - 3356

International Journal of
ELECTROCHEMICAL
SCIENCE
www.electrochemsci.org

Short Communication

Electrodeposition Synthesis of Au-ZnO Hybrid Nanowires and Their Photocatalytic Properties

Xue Zhao, Yongzhong Wu[*], *Xiaopeng Hao*[*]

State Key Laboratory of Crystal Materials, Shandong University, Jinan 250100, P.R. China
[*]E-mail: xphao@sdu.edu.cn, wuyz@sdu.edu.cn

Received: 27 January 2013 / *Accepted:* 15 February 2013 / *Published:* 1 March 2013

Au-ZnO hybrid nanowires have been successfully synthesized with assistance of AAO tempalte through a simple electrodeposition process. The samples were characterized by means of field-emission scanning electron microscopy (FESEM), energy dispersive X-ray spectrometer (EDS) and X-ray diffraction (XRD). The photocatalytic properties of the prepared Au-ZnO hybrid nanowires and individual ZnO nanowires were studied, and the Au-ZnO hybrid nanowires showed higher photocatalytic activity. The enhanced photocatalytic efficiency is attributed to the synergetic effect and unique charge-transfer kinetics in the as-prepared Au-ZnO hybrid nanowires.

Keywords: Au-ZnO hybrid nanowires; electrodeposition; photocatalytic; synergetic effect; charge-transfer

1. INTRODUCTION

One-dimensional nanostructures have attracted considerable attention in recent years owing to their unique structure and spectacular optical, electrical and magnetic properties [1-6]. They have played important roles in a wide range of applications such as nanoelectronics, optoelectronics, catalysis, plasmonics and biosensors [7-10]. Noble metal nanostructures, for example Au nanowires, have displayed high surface-enhanced Raman scattering (SERS) [11], localized surface plasmon resonance (LSPR) [12] and enhanced photocatalytic properties [13-14]. As an important II-VI semiconductor, ZnO nanostructure has made significant advances over the past years in optoelectronics devices, photocatalysis and biological applications [15-21] due to its unique properties.

The formation of one-dimensional hybrid nanostructures with tunable compositions has led to materials with multiple functionalities and unique properties not realized in single-component structures that are useful for a wide range of applications. Recently, noble metal-semiconductor hybrid nanostructures have been extensively studied because of their excellent optical, catalytic and electrical

properties. The band gap emission of ZnO can be greatly enhanced by synthesizing hybrid nanostructures of Au-coated ZnO nanowires [22-23]. The Au-coated ZnO nanostructures showed a good selectivity in biosensors and detection [21, 24] and have been applied to optoelectronic and energy harvesting devices [25-26].

Catalytic degradation of organic dye has attracted great attention due to their high toxicity to water resources. Metal-semiconductor hybrid nanostructures have exhibited excellent enhanced catalytic properties. The fabrication of uniform Ag-coated ZnO nanowires [27] with high catalytic activity was reported. M-Cu_2O (M = Ag, Au) heterogeneous nanocrystals were successfully prepared and showed enhanced photocatalytic activities. The noble metal nanoparticles deposited on the semiconductor surfaces may serve as electron sinks, promoting the separation of photo-induced electrons and holes, and thus increasing the photocatalytic efficiency [27]. Recently, Li's group [13] synthesized Au-ZnO hybrid nanopyramids based on a seed-mediated growth process showing enhanced photocatalytic activities. Although some progresses have been made in the synthesis of Au-ZnO hybrid nanostructures, most are focused on the Au nanoparticles-coated ZnO one-dimensional composite structures [28-29] or heterogeneous nanocrystals [13], less work has been done on the preparation of one-dimensional Au-ZnO hybrid nanowires. Moreover, the preparation of one-dimensional metal-semiconductor nanostructures was carried out mostly by combination of electrochemical deposition and CVD [30-31]. In our experiment, only electrodeposition was adopted in the synthesis of Au-ZnO hybrid nanowires.

Electrodeposition can be used to deposit metal, semiconductor or polymer into AAO templates and offers marked advantages over other methods for the synthesis of one-dimensional nanostructures. Electrodeposition synthesis is a simple method for the preparation of nanomaterials and the process has a low cost and high efficiency. It enables excellent control over the geometry and chemical compositions by changing the plating solution and varying the potential of the deposition. Electrochemical deposition does not require expensive instrumentation, high temperatures or low-vacuum pressures. Till now, electrodeposition has been one of the most successful methods of filling the AAO with well crystallized nanomaterials [32].

In this work, Au-ZnO hybrid nanowires with an Au nanorods-ZnO nanowires nanostructure were prepared within the AAO tempalte by simple electrochemical deposition. The photocatalytic activities of the as-prepared nanowires were investigated. And catalytic degradation activity of the Au-ZnO hybrid nanowires in the MO solution is higher than individual ZnO nanowires. The enhanced photocatalytic activity may be attributed to the synergetic effect and unique charge-transfer kinetics in the as-synthesized Au-ZnO hybrid nanowires. Furthermore, the homogeneous component of Au segments in the hybrid structures also plays a significant role in the photocatalytic process.

2. EXPERIMENTAL PROCEDURE

2.1. Synthesis procedure

The anodic aluminum oxide membranes (AAO) were purchased from Whatman, and the nominal diameter (d_N) is 100 nm specified by the manufacturer. A layer of gold film serving as back

electrode was electron-beam evaporated onto one side of the AAO membrane. A thick layer of Au was needed in case of the wide pores to ensure that the electrode completely covered the pores [33]. After evaporation, the membrane was fixed with the Au electrode facing down onto a conducting substrate (aluminum foil in our experiment) using an adhesive sticker. A bundle of Cu wires was applied to introduce the electrode to the deposition system. Nail polish was smeared on the aluminum foil and around the AAO to isolate electrolyte from undesired deposition. Electrodeposition was conducted in a Teflon cell by a three-electrode system. There was no separate compartment for the counter electrode which was a Pt plate, nor was there any stirring or heating. A saturated calomel electrode (SCE) was applied as reference electrode for the applied potential. Using a conventional potentiostat, the current was measured during electroplating at a fixed potential versus SCE, referred to as V_{SCE}.

All chemicals were commercially available and utilized as received without further purification unless otherwise stated. Au segments were grown from an electrolyte that contained 4 g L^{-1} $HAuCl_4 \cdot 4H_2O$ (99.99%, Alfa-Aesar) and 3.71 g L^{-1} H_3BO_3. Zn segments were deposited from 80 g L^{-1} $ZnSO_4 \cdot 7H_2O$ and 30 g L^{-1} H_3BO_3. The pH values of both electrolytes were adjusted to 3-4 by HNO_3. Au segments and Zn segments were separately deposited at constant potentials of -1.0 V and -1.5 V. After electrochemical deposition, the AAO membrane was removed in 20 g L^{-1} NaOH solution and the prepared sample was washed with distilled water for three times before drying. Due to protection of nail polish, the AAO was etched only from top-side of the nanowires, which could keep a good morphology of Au-Zn hybrid nanowires. The synthesized Au-Zn nanowires were then annealed at 300 ℃ for 50 h to obtain the desired Au-ZnO nanowires [34].

The photocatalytic properties of the as-prepared ZnO and Au-ZnO nanowires were evaluated by the photodegradation of methyl orange (MO) dye at room temperature. In a typical process, the prepared sample (with an area of 5 cm^2) was suspended in aqueous solutions of MO (60 mL, 20 mg L^{-1}) with constant stirring. The beaker was kept in the dark for 30 min to ensure the adsorption equilibrium before light irradiation. A 300 W Hg lamp (Kaifeng HXSEI Science Instrument Factory) was used as the light source. The efficiencies of the bleaching processes were evaluated by monitoring the dye decolorization at the maximum absorption around 463 nm as a function of irradiation time in the MO solution with a UV-visible spectrophotometer of Shimadzu UV 2550. Self-degradation of the MO dye solution under UV was encountered during the measurements.

2.2. Structural and morphological characterization

The hybrid nanowires were characterized by using field-emission scanning electron microscopy (FESEM， HITACHI S4800, Japan), energy dispersive x-ray spectrometer (EDS, HORIBA EMAX Energy EX-450, Japan) and X-ray diffraction (XRD, Bruker/D8-advance with Cu K_α radiation (λ = 1.54178 Å), Germany).

3. RESULTS AND DISCUSSIONS

Au-ZnO hybrid nanowires were fabricated by simple electrochemical deposition within the AAO template followed by annealing 50 h at 300 ℃. SEM and XRD patterns of the as prepared Au-Zn

nanowires are exhibited in Fig. 1a and b, respectively. The nanowires are well-ordered, uniform and with a high density, whose diameter and length are about 300 nm and 17 μm, respectively. The diffraction peaks in XRD pattern shown in Fig.

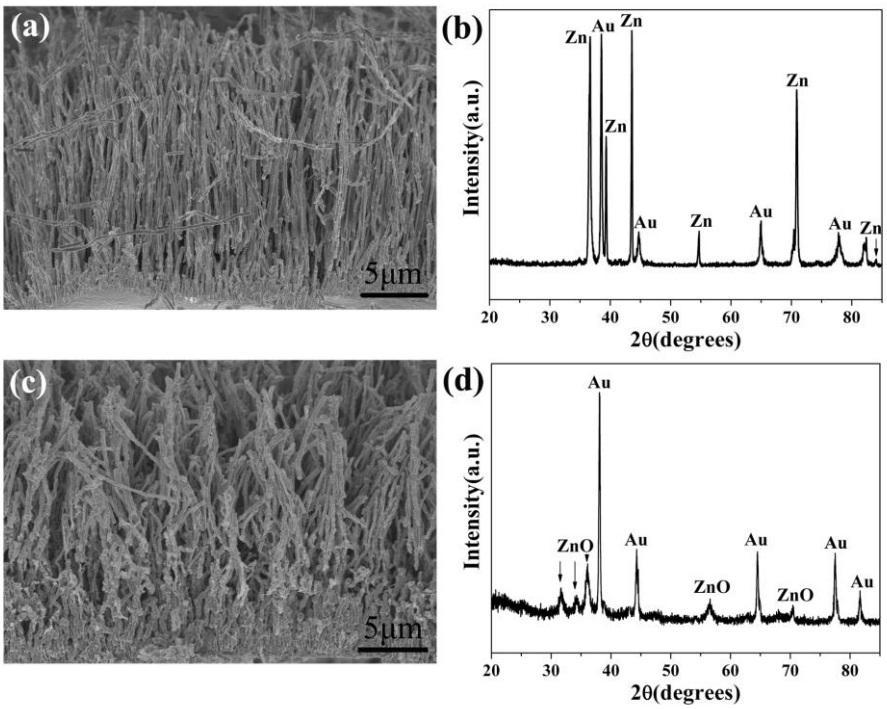

Figure 1. SEM images and XRD patterns of the products: (a), (b) Au-Zn hybrid nanowries; (c), (d) Au-ZnO hybrid nanowires

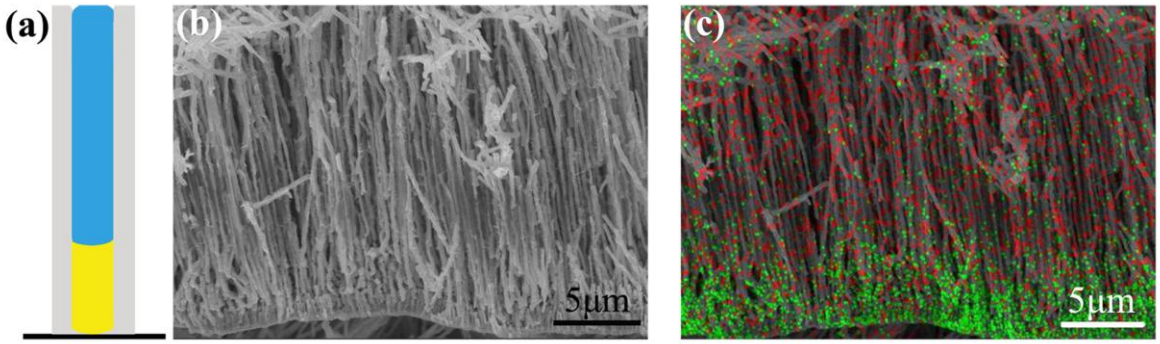

Figure 2. (a) Scheme of the as-prepared Au-Zn hybrid nanowires (b) FESEM image (c) EDS elemental distribution image of the Au-Zn hybrid nanowires

1b are indexed to cubic Au and hexagonal Zn which are in good agreement with standard JCPDS Cards (Au: Card No.04-0784; Zn: Card No.04-0831). After annealing, Zn segments in Au-Zn nanowires were oxidized and Au-ZnO hybrid nanowires were obtained as shown in Fig. 1c. The morphology of Au-ZnO is similar to that of the Au-Zn, but the connection sections of Au and ZnO segments are anamorphic to a certain extent after the anneal process. The reason for distortion is

supposed to be low melting point of Au segments when it is in nanometer scale. XRD test was carried out to confirm the ZnO structure. The diffraction peaks of Au and ZnO in Fig. 1d are in good agreement with standard JCPDS Cards (Au: Card No.04-0784; ZnO: Card No.36-1451), which are indexed to cubic Au and hexagonal ZnO.

EDS mapping spectrum was applied to prove the Au-Zn hybrid structures. Au-Zn nanowires shown in Fig. 2b were taken points for the EDS mapping, and the results are exhibited in Fig. 2c. The green and red dots are separately representative of the distribution of Au and Zn elements. The EDS elemental distribution map reveals that the nanowires are composed of two components, and the Au segments and Zn segments are about 5 μm and 12 μm in length, respectively. The illustration in Fig. 2a describes the Au-Zn hybrid nanowires schematically.

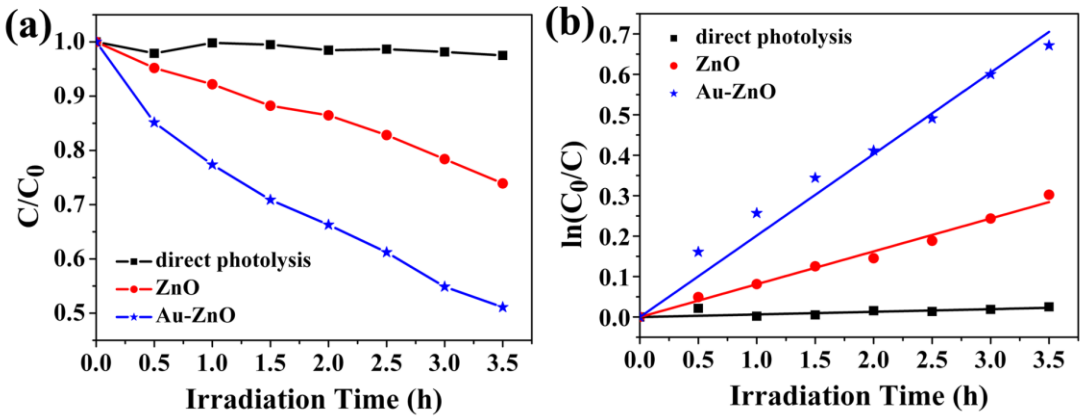

Figure 3. (a) The C_0/C vs. time curves of MO photodegradation using both kinds ZnO-based photocatalysts and (b) pseudo-first-order kinetic rate plots for the photocatalytic degradation

The photocatalytic activities were investigated by the degradation of MO dye under UV light irradiation as shown in Fig. 3. For comparison, the single-component of individual ZnO nanowires was chosen for testing, which was achieved by the same electrodeposition parameters as Au-ZnO nanowires. UV light irradiation of the MO/Au-ZnO solution system led to an apparent degradation of MO, and 49% decrease in the MO concentration in 3.5 h. The degradations of MO over ZnO nanowires and control experiments were also carried out. Only 26% MO was decomposed within 3.5 h in the MO/ZnO solution system and the MO dye solution without any photocatalyst accession decomposed only 2.5% over the same interval. Clearly, the Au-ZnO hybrid architectures show much higher photocatalytic activities than the single ZnO nanowires.

The reaction kinetics of the heterogeneous photocatalysis has been described by the Langmuir-Hinshelwood model [35-36]. According to this model, the photocatalytic degradation of the dye in the presence of the photocatalyst exhibits pseudo-first-order behaviour with respect to the concentration of the dye.

$$-\frac{d[C]}{dt} = K_{obs}[C] \qquad (1)$$

where K_{obs} is the pseudo-first-order reaction constant for the photocatalytic degradation of the MB dye. The Eq. (2) can be changed into

$$\ln(\frac{C_0}{C}) = K_{obs}t \qquad (2)$$

where the slope K_{obs} is the apparent reaction rate.

Based on the pseudo-first-order reaction, the UV degradation reaction rates of the as prepared nanowires were calculated. The UV degradation reaction rate of the Au-ZnO hybrid nanowires are 2.5 times and 30 times that of the ZnO nanowires and the pure MO system.

The enhanced photocatalytic activities may be mainly attributed to the synergetic effect and unique charge-transfer kinetics in the as-synthesized Au-ZnO hybrid nanowires [13]. Furthermore, the homogeneous component of Au nanowires in the hybrid structures plays a significant role in the photocatalytic process, and thus, exhibit higher photocatalytic efficiencies [37]. It is believed that catalytic enhancement is attributed to the synergetic effect that occurs at the interfaces of Au and ZnO segments [8]. The photocatalytic activities are enhanced by their extended link, and the larger interconnection area between Au and ZnO offers higher activity. The electronic structures of both the Au and the ZnO are modified by electron transfer across the interface. The polarization effect arises from the interfaces of Au and ZnO nanowires make ZnO more active, as a result, Au-ZnO hybrid nanowires exhibit the enhanced catalysis efficiency [38-39]. The Au-ZnO system shows unusual charge storage behavior. The photogenerated electrons get distributed between the ZnO and Au segments. Au possesses a unique property of storing electrons. The charge storage in the Au sections causes a large buildup of capacitance of the Helmoltz and diffuse double layer. The Fermi level of Au (0.4V vs NHE) is more positive than the conduction band of energy of ZnO (-0.5 V vs NHE at pH=7). The Fermi level becomes more negative with transfer of each electron into the Au segments. As the electrons get distributed between the ZnO and Au layers they attain Fermi-level equilibration [23]. The photo-generated electrons are stored in the Au segments and the recombination of the photo induced electron-hole pairs in the ZnO segments are thus reduced, which lead an enhancement in Au-ZnO hybrid nanowires [40].

4. CONCLUSIONS

In summary, Au-ZnO hybrid nanowires have been successfully synthesized by depositing Au nanorods followed by electrochemical deposition of Zn nanowires within AAO template through an annealing process. Electrodeposition is a simple method for the preparation of one-dimensional metal-semiconductor materials and the process has a low cost and high efficiency. Moreover, it does not require expensive instrumentation, low-vacuum pressures or high temperatures. The Au-ZnO hybrid

nanowires exhibit higher photocatalytic activity than the individual ZnO nanowires. Because of the unique structure and simple synthetic method, the as-prepared Au-ZnO hybrid nanowires are expected to provide new insights in optoelectronic devices, catalytic and biological applications. The electrodeposition synthesis may be a new method for the prepration of other hybrid structures.

ACKNOWLEDGMENTS
This work was financially supported by National Basic Research Program of China (2009CB930503), NSFC (Contract No. 51021062), the Fund for the Natural Science of Shandong Province (ZR2010EM020, ZR2010EM049) and IIFSDU (2012JC007).

References

1. J.J. Mock, S.J. Oldenburg, D.R. Smith, D.A. Schultz, S. Schultz, *Nano Lett,* 2 (2002) 465.
2. A.A. Umar, M.Y.A. Rahman, R. Taslim, *Int J Electrochem Sci,* 7 (2012) 8384.
3. S. Kim, S.K. Kim, S. Park, *J Am Chem Soc,* 131 (2009) 8380.
4. R.L. Zong, J. Zhou, Q. Li, B. Du, B. Li, M. Fu, X.W. Qi, L.T. Li, S. Buddhudu, *J Phys Chem B,* 108 (2004) 16713.
5. Z. Zhang, G. Meng, Q. Xu, Y. Hu, Q. Wu, Z. Hu, *J Phys Chem C,* 114 (2010) 189.
6. L. Piraux, J.M. George, J.F. Despres, C. Leroy, E. Ferain, R. Legras, K. Ounadjela, A. Fert, *Appl Phys Lett,* 65 (1994) 2484.
7. S. Park, S.W. Chung, C.A. Mirkin, *J Am Chem Soc,* 126 (2004) 11772.
8. J. Mu, C. Shao, Z. Guo, Z. Zhang, M. Zhang, P. Zhang, B. Chen, Y. Liu, *Acs Appl Mater Inter,* 3 (2011) 590.
9. K.M. Mayer, J.H. Hafner, *Chem Rev,* 111 (2011) 3828.
10. A.V. Kabashin, P. Evans, S. Pastkovsky, W. Hendren, G.A. Wurtz, R. Atkinson, R. Pollard, V.A. Podolskiy, A.V. Zayats, *Nat Mater,* 8 (2009) 867.
11. Q. Liao, C. Mu, D.-S. Xu, X.-C. Ai, J.-N. Yao, J.-P. Zhang, *Langmuir,* 25 (2009) 4708.
12. S. Habouti, M. Matefi-Tempfli, C.-H. Solterbeck, M. Es-Souni, S. Matefi-Tempfli, M. Es-Souni, *Nano Today*, 6 (2011) 12.
13. P. Li, Z. Wei, T. Wu, Q. Peng, Y. Li, *J Am Chem Soc,* 133 (2011) 5660.
14. Z. Wang, S. Zhao, S. Zhu, Y. Sun, M. Fang, *Crystengcomm,* 13 (2011) 2262.
15. Z.M. Yin, X.Y. Liu, Y.Z. Wu, X.P. Hao, X.G. Xu, *Opt Express,* 20 (2012) 1013.
16. X.H. Huang, J.B. Wu, Y. Lin, *Int J Electrochem Sci,* 7 (2012) 6611.
17. X.Y. Cao, L.J. Guo, J.P. Liu, *Int J Electrochem Sci,* 6 (2011) 270.
18. P. Tao, Q. Feng, J. Jiang, H. Zhao, R. Xu, S. Liu, M. Li, J. Sun, Z. Song, *Chem Phys Lett,* 522 (2012) 92.
19. J.B. Baxter, A.M. Walker, K. van Ommering, E.S. Aydil, *Nanotechnology,* 17 (2006) S304.
20. J.Z. Yin, Q.Y. Lu, Z.N. Yu, J.J. Wang, H. Pang, F. Gao, *Cryst Growth Des,* 10 (2010) 40.
21. Y. Wei, Y. Li, X. Liu, Y. Xian, G. Shi, L. Jin, *Biosens Bioelectron,* 26 (2010) 275.
22. H.Y. Lin, C.L. Cheng, Y.Y. Chou, L.L. Huang, Y.F. Chen, K.T. Tsen, *Opt Express,* 14 (2006) 2372.
23. B. Chen, H. Zhang, N. Du, D. Li, X. Ma, D. Yang, *Mater Res Bull,* 44 (2009) 889.
24. Y. Liu, M. Zhong, G. Shan, Y. Li, B. Huang, G. Yang, *J Phys Chem B,* 112 (2008) 6484.
25. S. Xu, Z.L. Wang, *Nano Res,* 4 (2011) 1013.
26. H. He, W. Cai, Y. Lin, B. Chen, *Langmuir,* 26 (2010) 8925.
27. X. Zhao, B. Zhang, K. Ai, G. Zhang, L. Cao, X. Liu, H. Sun, H. Wang, L. Lu, *J Mater Chem,* 19 (2009) 5547.

28. L. Sun, D. Zhao, Z. Song, C. Shan, Z. Zhang, B. Li, D. Shen, *J Colloid Interf Sci*, 363 (2011) 175.
29. J. Lee, H.S. Shim, M. Lee, J.K. Song, D. Lee, *J Phys Chem Lett*, 2 (2011) 2840.
30. G. Meng, F. Han, X. Zhao, B. Chen, D. Yang, J. Liu, Q. Xu, M. Kong, X. Zhu, Y.J. Jung, Y. Yang, Z. Chu, M. Ye, S. Kar, R. Vajtai, P.M. Ajayan, *Angew Chem Int Edit*, 48 (2009) 7166.
31. B. Chen, G. Meng, Q. Xu, X. Zhu, M. Kong, Z. Chu, F. Han, Z. Zhang, *Acs Nano*, 4 (2010) 7105.
32. S.J. Hurst, E.K. Payne, L.D. Qin, C.A. Mirkin, *Angew Chem Int Edit*, 45 (2006) 2672.
33. C. Schonenberger, B.M.I. van der Zande, L.G.J. Fokkink, M. Henny, C. Schmid, M. Kruger, A. Bachtold, R. Huber, H. Birk, U. Staufer, *J Phys Chem B*, 101 (1997) 5497.
34. Y. Li, G.W. Meng, L.D. Zhang, F. Phillipp, *Appl Phys Lett*, 76 (2000) 2011.
35. M. Logar, A. Kocjan, A. Dakskobler, *Mater Res Bull*, 47 (2012) 12.
36. H.S. Son, S.J. Lee, I.H. Cho, K.D. Zoh, *Chemosphere*, 57 (2004) 309.
37. C. Song, Y. Lin, D. Wang, Z. Hu, *Mater Lett*, 64 (2010) 1595.
38. C. Wang, H. Yin, S. Dai, S. Sun, *Chem Mater*, 22 (2010) 3277.
39. Y. Lee, M. Angel Garcia, N.A.F. Huls, S. Sun, *Angew Chem Int Edit*, 49 (2010) 1271.
40. V. Subramanian, E.E. Wolf, P.V. Kamat, *J Phys Chem B*, 107 (2003) 7479.